The Journal of Immunology

Sequence-Specific Alterations of Epitope Production by HIV Protease Inhibitors

Georgio Kourjian, Yang Xu, Ijah Mondesire-Crump, Mariko Shimada, Pauline Gourdain and Sylvie Le Gall

Supplementary Material	http://www.jimmunol.org/content/suppl/2014/03/07/jimmunol.130280 5.DCSupplemental.html
References	This article **cites 79 articles**, 31 of which you can access for free at: http://www.jimmunol.org/content/192/8/3496.full#ref-list-1
Subscriptions	Information about subscribing to *The Journal of Immunology* is online at: http://jimmunol.org/subscriptions
Permissions	Submit copyright permission requests at: http://www.aai.org/ji/copyright.html
Email Alerts	Receive free email-alerts when new articles cite this article. Sign up at: http://jimmunol.org/cgi/alerts/etoc

Sequence-Specific Alterations of Epitope Production by HIV Protease Inhibitors

Georgio Kourjian, Yang Xu, Ijah Mondesire-Crump, Mariko Shimada, Pauline Gourdain, and Sylvie Le Gall

Ag processing by intracellular proteases and peptidases and epitope presentation are critical for recognition of pathogen-infected cells by CD8$^+$ T lymphocytes. First-generation HIV protease inhibitors (PIs) alter proteasome activity, but the effect of first- or second-generation PIs on other cellular peptidases, the underlying mechanism, and impact on Ag processing and epitope presentation to CTL are still unknown. In this article, we demonstrate that several HIV PIs altered not only proteasome but also aminopeptidase activities in PBMCs. Using an in vitro degradation assay involving PBMC cytosolic extracts, we showed that PIs altered the degradation patterns of oligopeptides and peptide production in a sequence-specific manner, enhancing the cleavage of certain residues and reducing others. PIs affected the sensitivity of peptides to intracellular degradation, and altered the kinetics and amount of HIV epitopes produced intracellularly. Accordingly, the endogenous degradation of incoming virions in the presence of PIs led to variations in CTL-mediated killing of HIV-infected cells. By altering host protease activities and the degradation patterns of proteins in a sequence-specific manner, HIV PIs may diversify peptides available for MHC class I presentation to CTL, alter the patterns of CTL responses, and provide a complementary approach to current therapies for the CTL-mediated clearance of abnormal cells in infection, cancer, or other immune disease. *The Journal of Immunology*, 2014, 192: 3496–3506.

H ighly active antiretroviral therapy (HAART), which is a combination of nucleoside reverse transcriptase inhibitors (NRTIs), non-NRTIs (nNRT1s), protease inhibitors (PIs), and integrase inhibitors given to HIV-infected patients, efficiently suppresses HIV replication, leading to partial immune restoration and turning AIDS into a chronic disease (1).

HIV PIs block the HIV aspartyl protease, preventing the cleavage of HIV Gag and Pol polyproteins that include essential structural and enzymatic components of the virus. This blockage prevents the conversion of HIV particles into their mature infectious form (2). Currently, nine different HIV PIs are available on the market and used in HAART (3). Long-term treatment of responder patients with PI-containing HAART has been linked with several unpredicted adverse effects, such as hyperbilirubinemia, hyperlipidemia, or hypolipidemia (4), body fat redistribution (5), insulin resistance (6), osteopenia, and osteoporosis (7, 8); these adverse effects occur more so with first-generation PIs such as saquinavir or ritonavir than with newer PIs such as darunavir (9). The design of the first-generation

HIV PIs is based on the transition-state mimetic of the Phe-Pro bond, the major substrate of HIV-I protease (10). Evidence showing the ability of the 20S proteasome to cleave similar bonds (11) raised questions about possible interactions between HIV PIs and the proteasome catalytic sites.

Proteasomes play a key role in the degradation of full-length proteins and defective ribosomal products into peptides (12) that can be further shortened or degraded by cytosolic aminopeptidases and endopeptidases such as thimet oligopeptidase (13, 14) or tripeptidyl peptidase II (15). Some of these peptides are translocated by the TAP complex into the endoplasmic reticulum (ER), where they can be further trimmed by ER-resident aminopeptidases (ERAP1 or ERAP2) (16, 17) and, provided they contain appropriate anchor residues, loaded onto MHC class I (MHC-I) and displayed at the cell surface.

Epitopes can be solely produced by the proteasome or a combination of proteasomes and aminopeptidases and/or endopeptidases, although the sequence of degradation events leading to epitope production is poorly defined. Peptides produced during protein degradation can be subjected to hydrolysis by various peptidases, thus limiting the amount of peptides available for MHC-I presentation (18–20). The specificity of each peptidase is determined by length and motifs in the substrate. Proteasomes have the broadest cleavage capacity and often define the C terminus of extended epitopes because of frequent cleavages after hydrophobic residues (21).

Aminopeptidases cleave N-terminal extensions of peptides shorter than 16 aa and have well-defined hierarchy of cleavable residues and noncleavable residues (22–24) that influence the kinetics of production of adjacent epitopes (24). We showed that specific motifs within and outside epitopes determine the sensitivity of peptide to degradation by cytosolic peptidases, the kinetics of epitope production, and contribute to the amount of peptides available for presentation to CTL (18, 24, 25). In addition, differences in peptidase activities among cell types also influence the kinetics and amount of epitope produced (26). The combination of specific sequences

within proteins and intracellular peptidase hydrolytic activities shapes the kinetics of production and amount of peptides available for loading onto MHC-I. Therefore, natural or artificial variations in cellular peptidase activities may change the balance between production and further cleavage of peptides, enhancing or impairing the presentation of various MHC-I epitopes. For instance, the inhibition of the proteasome by *N*-acetyl-leucyl-leucyl-norleucinal or ERAP-1 knockout in mice altered the degradation of proteins and changed the repertoire of peptides presented on MHC-I molecules and CTL responses (27–29). The three HIV PIs ritonavir, saquinavir, and nelfinavir inhibit the activity of purified mouse or human 20S proteasomes and the proteasome activity in immortalized cells (30–32), causing intracellular accumulation of polyubiquitinated proteins (33, 34). In mice infected with lymphocytic choriomeningitis virus (LCMV) and treated with ritonavir, the cytotoxic immune response against two T cell epitopes of LCMV was reduced and prevented the expansion of LCMV reactive CTL (30). One possible explanation for these changes in CTL responses might be PI-induced alteration of proteasome activity leading to modification of epitope production. No study has assessed in human primary cells the effect of PIs on postproteasomal peptidases equally important in Ag processing, the link between PI-induced alterations of cellular peptidases, HIV protein degradation patterns, and HIV epitope presentation to CTL (when HIV replication is not fully inhibited by HAART) (35, 36), or the effect of PIs on the processing of other pathogens that HAART-treated patients may encounter during coinfection.

In this article, we investigate the effect of seven HIV PIs (saquinavir, ritonavir, nelfinavir, indinavir, atazanavir, darunavir, and lopinavir/ritonavir [Kaletra]) on proteasome and aminopeptidase activities of PBMCs. Our results showed that HIV PIs variably altered not only proteasomal but also aminopeptidase activities. Furthermore, using an in vitro epitope processing assay (25), we showed that HIV PIs changed HIV peptide degradation patterns, the cytosolic stability, and amount of epitopes produced. In addition, by measuring the lysis of PI-treated and HIV-infected cells by epitope-specific CTL, we found that HIV PIs variably altered the presentation of HIV epitopes and the recognition by CTL. Finally, we identified motifs whose cleavage is enhanced or reduced by HIV PIs, leading to increased or decreased production of neighboring epitopes.

Altogether, these results show that by variably altering cellular protease activities, HIV PIs modify HIV protein degradation patterns, epitope production, and presentation, leading to variations in CTL responses.

Materials and Methods

Preparation of antiretroviral drug stocks

The antiretroviral tablets used in this study were obtained from two sources: 1) National Institutes of Health AIDS Research and Reference Reagent Program (National Institute of Allergy and Infectious Diseases), or 2) the Massachusetts General Hospital Inpatient pharmacy. The following reagents were donated by the National Institutes of Health AIDS Reagent Program: indinavir, lamivudine, and nelfinavir. From the Massachusetts General Hospital inpatient pharmacy we obtained ritonavir, saquinavir, atazanavir sulfate, delavirdine, darunavir, and Kaletra. The purified form of the antiretroviral drugs was obtained from Selleckchem (ritonavir, lopinavir, and darunavir), Sigma (saquinavir), and Santa Cruz (nelfinavir). All drugs were dissolved in 100% DMSO. Kaletra was prepared by combining lopinavir and ritonavir with 5:1 ratio, respectively; subsequently, Kaletra concentrations mentioned in this article correspond to lopinavir amount. Stock solutions of 50 mM were kept at −20˚C, and fresh aliquots were used for each experiment.

PBMC isolation from donors

The use of buffy coats from anonymous blood donors was approved under Protocol No. 2005P001218 by the Partners Human Research Committee (Boston, MA). PBMCs were isolated from buffy coats (Massachusetts General Hospital, Boston, MA) by Ficoll-Hypaque (Sigma-Aldrich, St. Louis, MO) density gradient centrifugation. The needed amount of PBMCs for live cell proteolytic activity measurement was taken for immediate use, and the remaining PBMCs were used for cytosol extraction (25).

Measuring proteolytic activities in live cells or purified enzymes

Chymotryptic, tryptic, and caspase-like activities of proteasomes present in live PBMCs or purified PBMC proteasome obtained using the protocol described by Kisselev and Goldberg (37) were measured with specific fluorogenic substrates (50 μmol/L Suc-LLVY-Amc, 50 μmol/L BocLRR-Amc, and 75 μmol/L ZLLE-Amc, respectively; Bachem) (26, 29). Different amino acid cleavage activities required 5 μmol/L X-Amc substrate, where X represents any amino acid (26). Pan-caspase activity was measured using 50 μmol/L Ac-DEVD-AMC fluorogenic substrate. PBMCs, purified PBMC proteasomes, or purified aminopeptidase ERAP1 (obtained from R&D Systems) were pretreated with increasing drug concentrations for 30 min at 37˚C before adding the fluorogenic substrates. The specificity of the reaction was assessed by preincubating cells with inhibitors of proteasomes (MG-132; 10 μmol/L), aminopeptidases (Bestatin; 120 μmol/L), or pan-caspase (Z-VAD-FMK; 20 μmol/L). Digitonin was added to the cells at final amount of 0.0025% to facilitate the entry of the drugs and the substrates into the cells. The fluorescence was measured at 37˚C every 5 min for 5 h using a VICTOR X Multilabel Plate Reader (Perkin Elmer, Boston, MA).

Drug toxicity measurement assay

PBMCs at 500,000 cells/ml were incubated overnight with different PIs in 48-well plates. Cells were stained with annexin and 7-aminoactinomycin D (Annexin V APC Apoptosis Detection Kit I; BD Pharmingen), and the percentage of apoptotic and necrotic cells were determined by flow cytometry.

HIV epitope processing assay

A total of 2 nmol purified peptide (>95% pure; Massachusetts General Hospital peptide core facility) was degraded in 20 μg PBMC cytosol pretreated with different PIs for 30 min. The degradation reaction was stopped at various time points with 1% formic acid, and degradation products were analyzed by liquid chromatography tandem mass spectrometry (LC-MS/MS). Peptides present in the digestion mix were purified by TCA precipitation at each time point. Equal amounts of peptide degradation samples at different time points were injected into a Nano-HPLC (NanoLC Ultra; Eksigent) and online nanosprayed into an Orbitrap mass spectrometry (LTQ Orbitrap Discovery; Thermo) at a flow rate of 400 nl/min. A Nano cHiPLC trap column (200 μm × 0.5 mm ChromXP c18-CL 5 μm 120 Å; Eksigent) was used to remove salts and contaminants in the sample buffers. Peptides were separated in a Nano cHiPLC column (75 μm × 15 cm ChromXP c18-CL 5 μm 300 Å; Eksigent) over a gradient of 2–40% buffer B (buffer A: water w/0.1% formic acid; buffer B: acetonitrile w/0.1% formic acid) in 20 min. Mass spectra were recorded in the range of 370–2000 Daltons. In the tandem mass spectrometry mode, the eight most intense peaks were selected with a window of 1 Dalton and fragmented. The collision gas is helium and collision voltage is 35 V. Peaks in the mass spectra were searched against the source peptides databases with Proteome Discoverer (version 1.3; Thermo) and quantitatively analyzed. The integrated area of a peak generated by a given peptide is proportional to the relative abundance of the peptide present. Each degradation time point was run on the mass spectrometer at least twice.

Cytosolic peptide stability assay

A total of 2 nmol purified peptide (Massachusetts General Hospital peptide core facility; >95% pure) was degraded at 37˚C in 20 μg PBMC cytosol pretreated with different PIs for 30 min. The reaction was stopped with 1% formic acid at various time points. The degradation of the peptide was analyzed by reverse-phase HPLC (RP-HPLC; Waters) as described previously (18). The peptide corresponds to one peak whose amount is proportional to the surface under peak. One hundred percent corresponds to the surface under peak for each peptide at time 0. Peptides incubated at 37˚C in buffer without extracts are similarly analyzed.

CTL induced killing assay

HLA-matched B cells were incubated with PI for 30 min before being infected with vesicular stomatitis virus G glycoprotein (VSVg)–pseudotyped Gag-Pol-GFP–expressing or NL4.3 HIV-GFP–expressing in-house–made virus. Thirty-six hours postinfection, half of the cells was stained with HLA-A/B/C allophycocyanin (BD Biosciences) and analyzed by flow

cytometry for the infection percentage and the HLA-A/B/C surface expression level. The other half of the cells was incubated with epitope-specific CTL clones at E:T ratio of 4:1. All conditions were done in triplicates. Noninfected cells were pulsed 30 min with decreasing concentration of CTL-matched or nonmatched epitopes and subjected to CTL killing to test the CTL specificity. To measure cell death, we used Vybrant fluorescence-based cytotoxic assay kit (Invitrogen). Percentage specific lysis was determined by using the following formula: ([experimental release − spontaneous release]/ [maximum release − spontaneous release]) × 100%. Maximum release was determined by lysis of all target cells with detergent (5% Triton X-100), and spontaneous release was determined by incubating nontarget cells (not infected) with CTL (38).

Statistical analysis

Data were analyzed using GraphPad Prism 5 software.

Results

HIV PIs alter cellular proteasome and aminopeptidase activities

We first aimed to assess the effect of seven HIV PIs (saquinavir, ritonavir, nelfinavir, indinavir, atazanavir, darunavir, and Kaletra), one NRTI (lamivudine), and one nNRTI (delavirdine) on the main proteolytic activities—chymotryptic, tryptic, and caspase-like activities of proteasomes (i.e., cleaving after hydrophobic, basic, and acidic amino acids, respectively)—and aminopeptidase in freshly isolated PBMCs from at least six different HIV⁻ donors.

The concentrations of the PIs used in this study correspond to the level of PIs found in the plasma of ART-treated persons (39–43). Using annexin and 7-aminoactinomycin D staining as markers for apoptosis and necrosis, we detected no toxicity on PBMCs treated at therapeutic concentrations of PIs ranging from 5 to 20 μM (Supplemental Fig. 1A). Furthermore, pan-caspase activity measurement showed no caspase induction after PI treatment (Supplemental Fig. 1B). Each protease activity was measured with a fluorogenic substrate composed of a peptide specific for each proteolytic activity and a fluorogenic coumarin-derivative moiety (24, 37) (Fig. 1A). For each protease activity, fluorescence was measured over time, and the hydrolysis kinetics was calculated as the maximum slope of fluorescence emission after subtraction of fluorescence in the absence of cells. For each substrate, 100% represents the maximum slope of fluorescence emission by cells incubated with substrate and DMSO control.

The specificity of substrate cleavage was checked by preincubation of cells with cognate inhibitors of proteasome (MG132) or aminopeptidase (Bestatin). In the presence of the specific inhibitor (Bestatin), aminopeptidase activity was reduced by 20-fold compared with the control (maximum slope of 145.35 for control and 7.25 for Bestatin). Increasing concentrations of ritonavir (2.5–20 μM) reduced aminopeptidase activities by 1.11- to 1.73-fold, respectively (Fig. 1B).

The effects of each PI at increasing concentrations on all three proteasome and aminopeptidase activities were assessed (Fig. 1C). Chymotryptic activity of proteasome (Fig. 1C, *upper left panel*) was decreased upon saquinavir, ritonavir, nelfinavir, or Kaletra treatment by 1.23- to 2-fold. In contrast, indinavir increased the chymotryptic activity by 1.15-fold, and atazanavir or darunavir did not change it. Saquinavir and atazanavir increased the proteasomal caspase-like activity (Fig. 1C, *upper right panel*) by 1.15- to 1.9-fold, whereas ritonavir decreased it by 1.54-fold; unlike the latter, the activity was not affected by nelfinavir, indinavir, darunavir, or Kaletra. Saquinavir and nelfinavir increased the proteasomal tryptic activity (Fig. 1C, *lower left panel*) by 1.38- to 1.7-fold. Ritonavir increased the activity at low concentration (2.5 μM) by 1.39-fold and decreased tryptic activity at higher concentrations by 5.5-fold. Kaletra also decreased the proteasomal tryptic activity by 1.24-fold. Proteasome tryptic activity was not affected by indinavir, atazanavir, or darunavir.

Saquinavir, ritonavir, nelfinavir, and Kaletra decreased aminopeptidase activities (Fig. 1C, *lower right panel*) by 1.21- to 1.83-fold, but no change was seen upon indinavir, atazanavir, or darunavir treatment. Delavirdine (nNRTI) and lamivudine (NRTI) did not have any significant effect on the proteasomal and aminopeptidase activities (G. Kourjian, unpublished observations).

The effect of the PIs on chymotryptic, caspase-like, tryptic, and aminopeptidase activities was similar when using live PBMCs, purified PBMC proteasome, and aminopeptidase ERAP1 (Fig. 1D) or PBMC cytosolic extracts (G. Kourjian, unpublished observations). This shows that the alterations induced by PIs are specific and validate the use of PI-treated cellular extracts as one approach to assess the impact of PIs on the processing of epitopes.

These results show that saquinavir, ritonavir, nelfinavir, and Kaletra altered proteasomal activities in human primary cells in agreement with previous studies testing first-generation PIs on purified proteasomes or immortalized cell lines (31, 33). In addition, we showed that these four PIs inhibited aminopeptidase activities known to play an important role in defining the composition of MHC-I peptide repertoire (17). Indinavir, atazanavir, and darunavir, the newer PIs, as well as reverse transcriptase inhibitors lamivudine and delavirdine, did not significantly affect peptidase activities tested in PBMCs.

Peptide degradation patterns are altered by HIV PIs

To assess the effect of HIV PI on peptide degradation patterns and epitope production, we used PBMC cytosolic extracts to degrade 3ISW9 (HQAISPRTLNAW) fragment, which is a precursor of an HLA-B57–restricted ISW9 epitope (ISPRTLNAW, aa 15–23 in Gag p24) that elicits frequent CTL responses in HLA-B57 HIV-infected individuals (18). Fig. 2A shows degradation products of substrate 3ISW9 identified by LC-MS/MS after a 60-min degradation in PBMC extracts in the absence of PIs. They included peptides encompassing epitope ISW9, termed precursors, optimal epitope ISW9, and peptides containing only part of the optimal peptide that will not bind to HLA-B57, termed antitopes.

To assess and compare the production of all peptides over time in each condition, we calculated the contribution of each peptide to the degradation products detected at a given time point. We first checked that the amount of peptide injected on the mass spectrometer directly correlated with the surface of the peptide's corresponding peak (Supplemental Fig. 2A, 2B). Three peptides were mixed at various ratios while keeping the total femtomole constant. The total intensity of all peaks was constant (<10% variation among mixes), and for each peptide the peak surface was proportional to the amount of the peptides (Supplemental Fig. 2C), thus validating the measurement of the relative contribution of each peptide to the total intensity of degradation peptides in the presence of various drugs. In PBMC extracts treated with 10 μM ritonavir or Kaletra, 3ISW9 degradation started slower compared with DMSO control or saquinavir-treated extracts (71–75 versus 43–55% 3ISW9 remaining at 10 min). However, the production of ISW9 was increased by 4.6- or 3.36-fold at 60 min upon ritonavir or Kaletra treatment, respectively (14 and 10% of total peptides upon ritonavir and Kaletra, respectively, compared with 3% in control; Fig. 2B–D), suggesting that peptide trimming was shifted toward epitope production. Saquinavir treatment of 10 μM produced 3.3-fold less ISW9 and 1.8-fold more antitopes compared with the control, suggesting that in the presence of saquinavir, precursors are being cut into peptides destroying epitopes (Fig. 2C). These changes in the ratios of categories of peptides were confirmed by comparing individual fragment intensities in the presence of various PIs. For instance, upon saquinavir treatment, the antitope QAISPRTL was produced up to 4-7-fold more than in control or Kaletra treatment, whereas
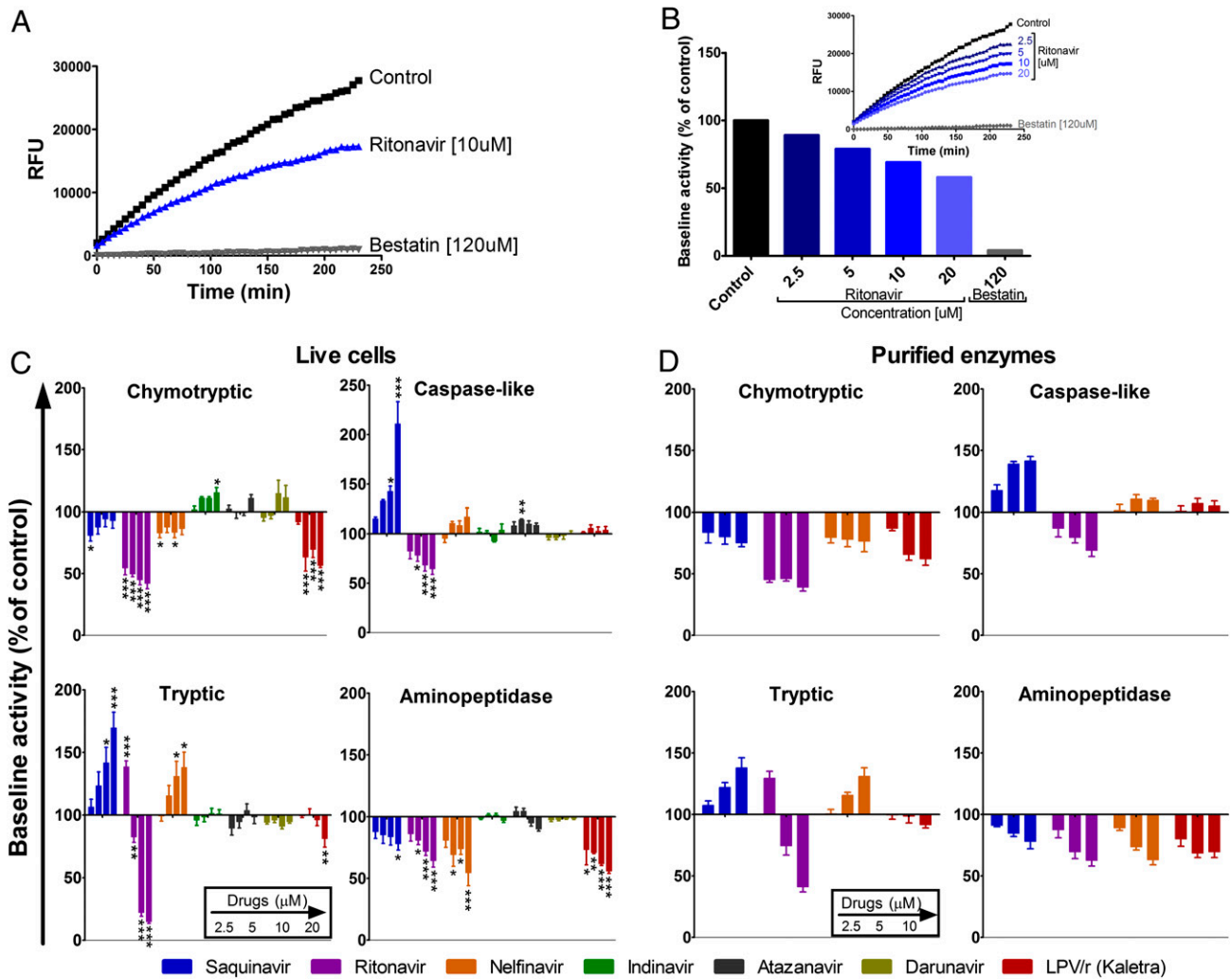
FIGURE 1. HIV PIs variably alter proteasome and aminopeptidase activities in human PBMCs. (**A**) Aminopeptidase substrate Leu-amc was added to PBMCs pretreated with DMSO (control, squares), 10 μM ritonavir (triangles), or 120 μM Bestatin (inverse triangles) and incubated for 4 h at 37°C, during which fluorescence emission was monitored every 5 min. (**B**) PBMCs were preincubated with increasing concentrations of ritonavir or 120 μM Bestatin before addition of Leu-amc. The maximum slope of fluorescence emission over 1 h was calculated for each condition. One hundred percent represents the maximum slope of fluorescence emission of the control (153.9). Maximum slope of fluorescence upon each treatment was compared with control. (**C**) PBMCs or (**D**) purified proteasomes or ERAP1 were pretreated with DMSO (control) or increasing concentrations of each PI (saquinavir, ritonavir, nelfinavir, indinavir, atazanavir, darunavir, and Kaletra [left to right bars on each graph]) before adding specific substrate for each activity (chymotryptic and caspase-like [*top panels*], tryptic and aminopeptidase [*lower panels*]). In each panel, 100% represents the maximum slope of DMSO-treated PBMCs (1161.8 for chymotryptic, 194 for caspase-like, 475 for tryptic, and 1063.6 for aminopeptidase) or purified proteasomes or ERAP1 (186.8 for chymotryptic, 27.1 for caspase-like, 91.8 for tryptic, and 507 for aminopeptidase). The maximum slope of treated PBMCs was compared with that of control. Average of six to eight healthy donors. *$p < 0.05$, **$p < 0.01$, ***$p < 0.001$, one-way ANOVA with Dunnett's posttest.

2-ISW9 (QAISPRTLNAW) precursor was produced at least twice less (Fig. 2E, 2F), suggesting that in the presence of saquinavir, precursors are being cut to antitopes from the C-terminal side (or overtrimmed from the N-terminal side), whereas in the presence of ritonavir or Kaletra, they are preferentially trimmed to epitopes. Two other epitopes are present in substrate 3ISW9: HLA-A25–restricted QW11 (QAISPRTLNAW) and HLA-B15–restricted HL9 (HQAISPRTL). In contrast with their positive effect on B57-ISW9 production, ritonavir and Kaletra reduced the production of A25-QW11 and B15-HL9 epitopes, suggesting that the effect of HIV PIs on epitope production is variable and peptide dependent (Supplemental Fig. 3). We had previously shown that variations in epitope production (caused by mutations or variations in peptidase activities) measured by mass spectrometry correlated with changes in CTL-mediated killing of infected cells endogenously processing and presenting HIV epitopes (18, 24, 25). Altogether, these results indicate that HIV PIs differently altered peptide degradation patterns, resulting in increased or de-creased epitope production and changing the ratio of cytosolic peptides available for loading onto MHC-I.

The intracellular stability of optimal HIV epitopes is altered upon HIV PI treatment

Peptides produced during protein degradation can be subjected to hydrolysis by multiple cytosolic proteases, thus altering the amount of peptides available for MHC-I presentation. The cytosolic stability of peptides is highly variable, defined by specific motifs, and contributes to defining the amount of peptides displayed to CTL (18, 19, 44). We hypothesized that PIs -by variably altering intracellular peptidase activities- might modify the cytosolic stability of peptides and consequently peptide availability for MHC-I loading.

To test the effect of HIV PI on the intracellular HIV epitope stability, we incubated highly purified peptides with cytosol from healthy human PBMCs pretreated with DMSO (control) or HIV PIs. The amount of peptide remaining over time was measured by
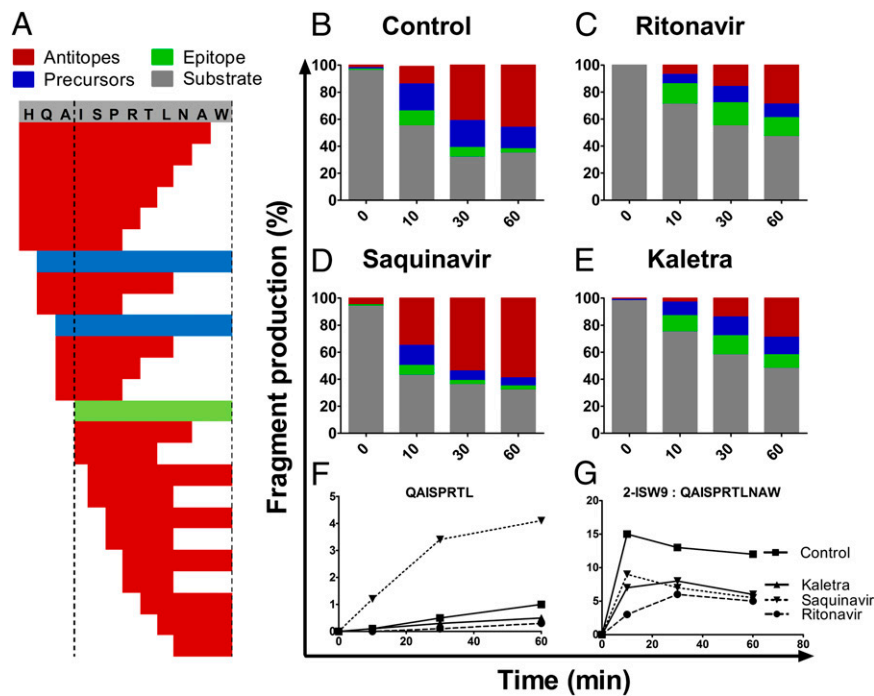
FIGURE 2. HIV PIs alter peptide degradation patterns. 3ISW9 (HQAISPRTLNAW) peptide containing HLA-B57–restricted ISW9 epitope (ISPRTL-NAW) was degraded in PBMC cytosolic extracts preincubated with DMSO (**A** and **B**) or 10 μM ritonavir (**C**), saquinavir (**D**), or Kaletra (**E**). Resulting degradation products at 0, 10, 30, and 60 min were analyzed by LC-MS/MS. Degradation peptides were categorized as substrate 3-ISW9 (gray), epitope ISW9 (green), precursors—peptides that include the epitope (blue) or antitopes (peptides including only part of the epitope (red) (A–E). Each peptide identified by a specific mass and charge corresponds to a peak of a specific intensity, and the proportion of each category of peptides to the total peak intensity (ranging from 7.1E+8 to 8.4E+8 at a given time point) was calculated at each time point in the presence of DMSO (B), ritonavir (C), saquinavir (D), or Kaletra (E). Percentage of antitope QAISPRTL (**F**) and precursor 2-ISW9 (QAISPRTLNAW) (**G**) production over time upon PI treatment. Figure is representative of one of three independent experiments using PBMC extracts from three different donors and run in duplicates on the mass spectrometer.

RP-HPLC profile analysis, where each peak defined by its elution time represents one peptide, and the surface area under the peak is proportional to the amount of peptide (25). The degradation of the peptide results in reduction of its peak and the appearance of additional peaks corresponding to truncated peptides. A value of 100% was assigned to the amount of input peptide present at time 0, and the amount of peptides remaining was calculated at each time point. The time at which 50% of the peptide was degraded defines its half-life. Fig. 3A illustrate the degradation rates of HLA-A02–restricted SL9 (SLYNTVATL, aa 77–85 in Gag p17) in extracts preincubated with control DMSO, saquinavir, or nelfinavir. Pretreating PBMC cytosol with saquinavir decreased SL9 degradation rate, thus increasing its half-life to 52 min (compared with 37 min in control), whereas nelfinavir treatment increased SL9 degradation and reduced its half-life to 24 min (Fig. 3A). We measured the half-life of five optimally defined HIV epitopes that elicit frequent CTL responses in HIV-infected persons in the presence or absence of 2 or 5 μM HIV PIs: HLA-A02–restricted SL9, HLA-A11–restricted ATK9 (AIFQSSMTK, aa 158–166 in reverse transcriptase of HIV-1 polymerase), HLA-B57–restricted KF11 (KAFSPEVIPMF, aa 30–40 in Gag p24), HLA-B57–restricted ISW9, and HLA-B57–restricted TW10 (TSTLQEQIGW, aa 108–117 in Gag p24) (45). The half-lives of these epitopes in untreated cytosol, which were highly variable (119.4, 37.2, 33.9, 25.7, and 14.8 min for TW10, ATK9, SL9, KF11, and ISW9, respectively) as we previously showed (18), was compared with their half-lives upon different PI treatments. A02-SL9 epitope half-life was increased by 1.4- ($p < 0.001$) and 1.2-fold ($p < 0.05$) by saquinavir and ritonavir, respectively, whereas nelfinavir and atazanavir reduced it by 1.25- ($p < 0.05$) and 1.33-fold ($p < 0.01$), respectively (Fig. 3B). Darunavir did not change the half-life of SL9 and four other peptides. B57-KF11 half-life was increased

by 1.44- ($p < 0.05$) and 1.52-fold ($p < 0.05$) by saquinavir and ritonavir, respectively (Fig. 3C). No other tested drug showed any effect on B57-KF11 half-life. B57-ISW9 half-life was increased by 1.48-fold ($p < 0.05$) by saquinavir (Fig. 3D). Other PIs tested did not significantly change B57-ISW9 half-life. A11-ATK9 and B57-TW10 half-life was not changed by any of the PIs tested (Fig. 3E, 3F). These results demonstrate that HIV PIs, by changing activities of cellular proteases, modified the cytosolic stability of several HIV epitopes, thus increasing or decreasing their availability for transfer into the ER, loading onto MHC-I, and display to CTL.

HIV PIs alter HIV epitope processing and presentation by HIV-infected cells to CTL

Having demonstrated that HIV PIs modified the degradation patterns of long peptides into epitopes and the intracellular stability of epitopes (two parameters that we previously identified to be critical to define the amount of MHC-bound peptides available for CTL recognition) (18, 24, 25), we next assessed whether HIV PIs could affect the endogenous processing and presentation of HIV epitopes and the subsequent CTL-mediated killing of HIV-infected cells. Because HIV PIs affect the late stages of replication, we performed single-round infections with nonreplicative virus to monitor epitope presentation. Upon PI treatment, single-round infection with either VSVg-pseudotyped lentivirus expressing HIV-1 Gag, Pol, and GPF or VSVg expressing HIV-1 NL4.3 without Env led to similar infection rates (67.3–68.5%) and did not affect the surface expression of HLA-A/B/C (mean fluorescence intensity ≈60; Supplemental Fig. 4). The PIs blocked the replication and release of HIV-1 NL4.3 in Jurkat cells, confirming the stability and the activity of the PIs (data not shown).
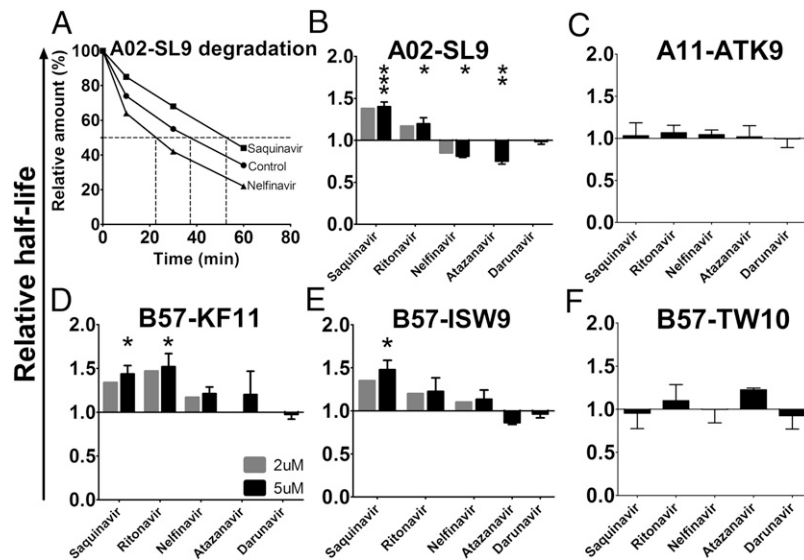
FIGURE 3. HIV PIs variably alter intracellular HIV epitope stability. (**A**) HLA-A02–restricted SL9 epitope (SLYNTVATL, aa 77–85 in HIV-1 Gag p17) was degraded in PBMC extracts pretreated with DMSO (control, circles), 5 μM nelfinavir (triangles), or 5 μM saquinavir (squares). Remaining peptide was quantified by RP-HPLC analysis after 0, 10, 30, and 60 min. One hundred percent represents the amount of peptide at time 0 calculated as the surface under the peptide peak detected by RP-HPLC (815.986, 821.569, and 813.118 for DMSO, saquinavir, and nelfinavir, respectively). Times at which 50% of the SL9 peptide remained correspond to peptide half-lives (37, 52, and 24 min for control, saquinavir, and nelfinavir, respectively). (**B–F**) HLA-A02–SL9 (B), HLA-B57-KF11 (C), HLA-B57-ISW9 (D), HLA-B57-TW10 (E), and HLA-A11-ATK9 (F) epitopes were degraded in PBMC extracts pretreated with DMSO, 2 μM PI, or 5 μM PI (saquinavir, ritonavir, nelfinavir, atazanavir, or darunavir). The cytosolic half-lives in control condition were 33.87, 25.66, 14.83, 119.4, and 37.21 min for SL9, KF11, ISW9, TW10, and ATK9, respectively. Fold differences of each epitope half-life upon treatment compared with control are presented in each panel. All data represent the average of four different experiments using four different PBMC extracts. $*p < 0.05$, $**p < 0.01$, $***p < 0.001$, one-way ANOVA with Dunnett's posttest.

HLA-matched B cell lines were pretreated with DMSO or 5 μM PI before being infected with either VSVg-pseudotyped lentivirus expressing HIV-1 Gag, Pol, and GPF or VSVg expressing HIV-1 NL4.3 without Env and used as targets in a fluorescence-based killing assay with various epitope-specific CTL clones (38). Killing is monitored with an extracellular fluorogenic substrate that fluoresces after cleavage by an intracellular enzyme released by dying cells (46). Fluorescence is monitored every 5 min after addition of CTL to target cells, allowing for real-time measurement of CTL-mediated killing in conditions where the percentage lysis at 4 h is similar to those obtained in Cr-based killing assay (38). HIV PIs did not affect CTL-mediated lysis of uninfected cells pulsed with various amounts of cognate peptides, in accordance with the lack of effect of PIs on MHC-I expression (Supplemental Fig. 4) and absence of toxicity on CTL (G. Kourjian, unpublished observations). Fluorescence emission after synchronized addition of B57-KF11 or B57-ISW9 CTL to HIV-infected B57 expressing B cells was similar, indicative of similar kinetics of killing of infected targets by the two clones recognizing these two p24 epitopes (Fig. 4A). However, preincubation of target cells with ritonavir before infection had opposite effects on the kinetics of killing by the two CTL clones. The kinetics of killing by B57-KF11 CTL was slower and the maximum lysis reduced upon ritonavir treatment, whereas they were enhanced for B57-ISW9 CTL (Fig. 4A). We compared the specific lysis of HLA-B57 HIV-infected B cells 4 h after parallel addition of three B57-restricted, Gag-specific CTL clones in the presence of various PIs (Fig. 4B–D), and similarly the killing of A03/11 HIV-infected B cells by A03 Gag-specific or A11-restricted RT-specific CTL (Fig. 4E–F). Saquinavir, ritonavir, nelfinavir, and indinavir reduced the killing of HIV-infected cells by the B57-KF11 CTL by 1.31-fold ($p < 0.05$), 2.4-fold ($p < 0.001$), 2.44-fold ($p < 0.001$), and 1.9-fold ($p < 0.001$), respectively (Fig. 4B). The killing of HIV-infected cells by B57-ISW9 CTL was inhibited 2.44-fold ($p < 0.001$) and 1.2-fold ($p < 0.05$) by saquinavir and

nelfinavir, respectively (Fig. 4C). In contrast, ritonavir increased it by 1.2-fold ($p < 0.05$) and nelfinavir had no effect. The lysis of HIV-infected cells by B57-TW10 CTL was decreased only by nelfinavir (1.46-fold, $p < 0.05$; Fig. 4D). None of the drugs tested altered the recognition and killing of HIV-infected cells by A03-RK9 CTL, an epitope that is efficiently produced and highly stable in the cytosol (18, 25) (Fig. 4E). The killing of HIV-infected cells by A11-ATK9 CTL, which was lower due to the lesser amount of RT present in incoming virions compared with Gag, was reduced by saquinavir, ritonavir, nelfinavir, and indinavir by 8-fold ($p < 0.01$), 4-fold ($p < 0.01$), 4.8-fold ($p < 0.01$), and 3-fold ($p < 0.01$), respectively (Fig. 4F). These results show that HIV PIs altered the endogenous processing and the presentation of HIV epitopes to CTL in various ways and underscore the link between drug-induced alterations of epitope production and subsequent changes in epitope-specific CTL responses. Ritonavir enhanced both in vitro production and intracellular stability of ISW9 (Figs. 2C, 3D), and led to enhanced killing of infected cells that endogenously processed ISW9, whereas the reduced in vitro production of ISW9 in the presence of saquinavir correlated with the reduced killing of HIV-infected cells by B57-ISW9 CTL. Therefore, PI-induced modulations of cellular peptidase activities leading to changes in peptide degradation patterns, epitope production, or intracellular peptide stability affected epitope presentation and recognition of HIV-infected cells by CTL.

HIV PIs variably modify the cleavage of amino acids, resulting in sequence-specific alterations of epitope production

Because HIV PIs variably affected the activities of cellular peptidases and the processing and presentation of epitopes in different ways, we hypothesized that alterations induced by PIs may be sequence specific. To individually test the impact of each PI on amino acid cleavage, we measured the hydrolysis of fluorogenic substrate X-amc (where X can be any amino acid) in PBMCs pretreated with 10 μM of various PIs. We compared the hydrolysis of 17 aa in
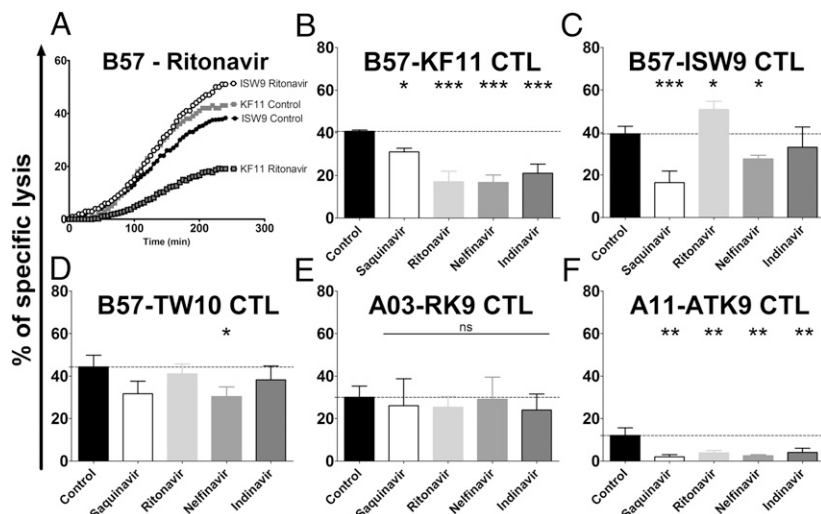
FIGURE 4. HIV PIs variably alter the endogenous processing and presentation of HIV epitopes by infected cells to CTLs. (**A**) HLA-B57 B cells were treated with DMSO or 5 μM ritonavir before being infected with VSVg-NL4.three-dimensionalEnv and used as targets in a fluorescence-based killing assay with KF11- and ISW9-specific CTLs. Fluorescence emission was recorded every 5 min from the moment ISW9-specific (circles) or KF11-specific (squares) CTLs were added to HIV-infected cells pretreated with DMSO (no line) or with ritonavir (black lines). Specific lysis was calculated as [(CTL-induced release − spontaneous release)/(maximum release − spontaneous release)] × 100%. Maximum release was determined by lysis of all target cells with detergent (5% Triton), and spontaneous release was determined by incubating noninfected cells with CTLs. (**B–F**) HLA-matched B cells were treated with DMSO (control; black bars) or 5 μM PI (saquinavir, ritonavir, nelfinavir, atazanavir, or darunavir) before being infected with VSVg-NL4.three-dimensionalEnv and used as targets in fluorescence-based killing assay with (B) KF11-, (C) ISW9-, (D) TW10-, (E) RK9-, or (F) ATK9-specific CTLs. The lysis percentage of target cells at 4 h after addition of an epitope-specific CTL was compared among cells pretreated with indicated PIs or DMSO control. All data represent the average of four experiments. *$p < 0.05$, **$p < 0.01$, ***$p < 0.001$, one-way ANOVA with Dunnett's posttest.

PBMCs pretreated with saquinavir, ritonavir, nelfinavir, Kaletra, or control DMSO (Fig. 5A). The hydrolysis of 13 aa was inhibited by 1.2- to 2.5-fold. Twelve of 13 aa corresponded to substrates cleavable by aminopeptidases (24). The inhibition of their hydrolysis by HIV PIs is similar to that observed in Fig. 1C using the standard leucine-amc substrate. The cleavage of Proamc performed by prolylpeptidases, but not by aminopeptidases (47), was also reduced, suggesting that these PIs can also inhibit prolylpeptidase activities. In contrast, the hydrolysis of glutamic acid, aspartic acid, glutamine, and asparagine, substrates not cleavable by aminopeptidases, was increased, on average, by 2.2-, 1.3-, 1.35-, and 1.4-fold, respectively (Fig. 5A), becoming as cleavable as valine and other residues slowly cleavable in the cytosol. Thus, by modifying the cleavage of various amino acids in opposite ways, certain PIs may change the patterns of peptide degradation in the cytosol. To test the relevance of these residue-specific changes on epitope processing, we measured the production of an HIV epitope flanked by residues whose cleavage was either reduced (isoleucine, I) or enhanced (glutamic acid, E) by PIs. The processing of this epitope is proteasome and aminopeptidase dependent, and we previously showed that the trimming efficiency of extended KF11 (VXX-KF11) into KF11 correlated with that of fluorogenic X-amc (24). We compared the degradation of peptide 3KF11 (VEEKAFSPEVIPMF), which is a precursor of HLA-B57–restricted KF11, with that of an artificial mutant 2I-3KF11 (V<u>II</u>KAFSPEVIPMF), in the presence or absence of 10 μM ritonavir. In the absence of PI, the degradation rates of 3KF11 and 2I-3KF11 proceeded with similar kinetics over 60 min, although, on average, 3.4-fold more epitope (KF11) and less 1KF11 precursors were produced from 2I-3KF11 because of faster N-terminal trimming of isoleucine compared with glutamic acid as we previously reported (24) (Fig. 5B). However, upon ritonavir treatment, 3KF11 degradation produced less precursors (on average, 1.8-fold less for EEKAFSPEVIPMF and 1.4-fold less for EKAFSPEVIPMF) and 1.5-fold more epitopes compared with the control (Fig. 5C, *upper panels*), suggesting that ritonavir, by

increasing the hydrolysis of glutamic acid, increased the trimming of precursors toward epitope KF11. In contrast, during 2I-3KF11 degradation, because of the decreased hydrolysis of isoleucine upon ritonavir treatment, the trimming of 2I-3KF11 toward epitopes was inhibited, resulting in increased amounts of precursors (on average, 1.6-fold more for IIKAFSPEVIPMF and 1.8-fold more for IKAFSPEVIPMF) and 1.46-fold less epitopes (Fig. 5C, *lower panels*). These opposite variations in in vitro production of KF11 (from 1.8-fold more to 1.5-fold less) fell within the range that affected endogenous processing and presentation of KF11 to CTL in our previous study (24). Together, these results indicate that the effect of PI on peptide degradation is sequence specific, thus increasing the production of some epitopes and decreasing the production of others, and modifying the ratios of peptides available for loading onto MHC-I and presentation to CTL.

Discussion

The ability of CTL to clear virus-infected cells is dependent on the processing of viral Ags by cellular proteases and peptidases and peptide display by MHC-I. Any perturbation of cellular peptidase activity could modify protein degradation patterns and consequently epitope presentation. In this study, we showed that several HIV PIs, by changing not only cellular proteasome but also aminopeptidase activities, altered HIV Ag degradation patterns and cytosolic stability of peptides in a sequence-specific manner, leading to variations in lysis of HIV-infected cells by CD8+ T cells.

Four of seven PIs affected at least one cellular peptidase activity. Saquinavir could either enhance or reduce proteasome and aminopeptidase hydrolytic activities, whereas other PIs such as Kaletra mostly reduced proteasome and/or aminopeptidase activities, suggesting different interactions between each drug and each cellular enzyme. It was previously shown using molecular docking that ritonavir can bind to the active center of the yeast proteasome PRE2 subunit that is homologous to human proteasome β5 subunit (48), elucidating the inhibition of the chymotryptic activity by ritonavir (30, 48, 49).
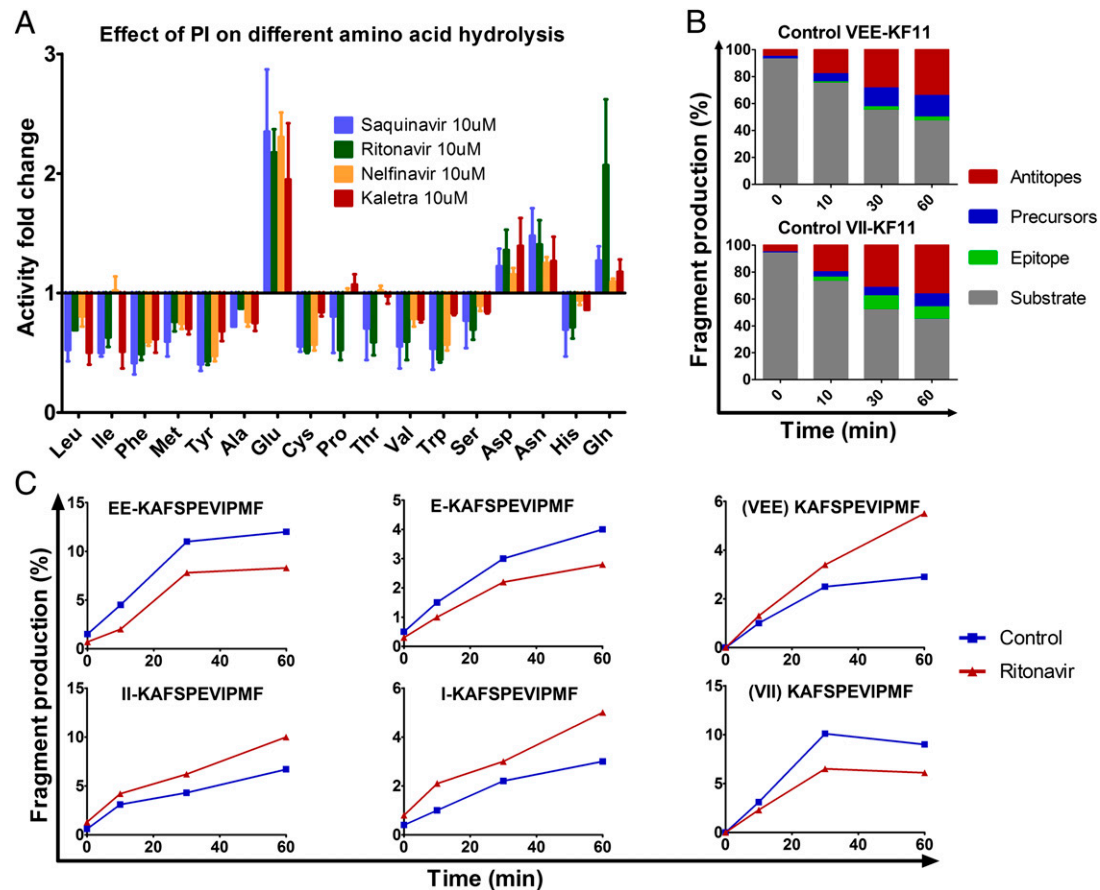
FIGURE 5. HIV PIs modify HIV peptide degradation in a sequence-specific manner. (**A**) The hydrolysis of various amino acids was measured with fluorogenic substrate in PBMCs pretreated with 10 μM saquinavir (blue), ritonavir (green), nelfinavir (yellow), or Kaletra (red). Fluorescence emission was measured over 1 h, and the maximum slope of fluorescence was measured in each condition. The fold difference of the maximum slope of PI-treated PBMCs over DMSO control was calculated for each condition. Data represent average results of four different experiments using four different PBMC donors. (**B**) The 3KF11 (VEEKAFSPEVIPMF, *upper panel*) and 2I-3KF11 (VIIKAFSPEVIPMF, *lower panel*) peptides were degraded using PBMC extracts. The resulting degradation products were analyzed by LC-MS/MS at 0, 10, 30, and 60 min. The distribution of substrate (3KF11 or 2I-3KF11, in gray), epitope (KF11, in green), precursors (blue), or antitopes (red) is shown at each time point. (**C**) The relative amount of epitope precursors (EEKAFSPEVIPMF and EKAFSPEVIPMF) and epitope KF11 (*upper panels*), and 2I-3KF11 epitope precursors (IIKAFSPEVIPMF and IKAFSPE-VIPMF), and epitope (*lower panels*) were calculated at each time point of degradation with extracts pretreated with DMSO (control, blue) or with ritonavir (red). (B and C) One experiment representative of two independent experiments using PBMC extracts from two different donors and run in duplicate on the mass spectrometer.

Likewise, HIV PIs might interact with noncatalytic effector sites in the proteasome and aminopeptidases that were shown in enzymatic studies to regulate the different catalytic activities (50–52). This would provide a potential mechanism of either inhibition or enhancement of cellular peptidases by HIV PIs, although molecular modeling and structural studies are required to test this hypothesis.

First-generation PIs like ritonavir, saquinavir, and nelfinavir showed stronger effect on proteasome and aminopeptidase activities than newer PIs like atazanavir and darunavir. First-generation PIs induced more rapid and profound adverse effects on lipid and glucose metabolism than did newer PIs (4, 7, 8, 53–55). Rats treated with ritonavir developed hyperlipidemia and displayed higher RNA expression of proteasome subunits (56, 57). Although there is no clear mechanistic link between the two observations, ritonavir-induced proteasome inhibition may trigger a feedback loop leading to increased proteasome expression as observed with proteasome inhibitors (58). PI-induced proteasome inhibition may modify the half-life of proteins involved in glucose or lipid metabolism, such as the documented accumulation of sterol regulatory binding proteins 1/2 inducing constitutive lipid biosynthesis

in mice (59). Whether the modification of intracellular aminopeptidase activities would affect glucose or lipid metabolism remains unknown. Surface aminopeptidases such as membrane-bound ectoenzyme aminopeptidase N/CD13 or intracellular aminopeptidases trafficking to the surface such as insulin-responsive aminopeptidase are involved in peptide cleavage, cholesterol uptake for aminopeptidase N (60, 61), or glucose transport uptake for insulin-responsive aminopeptidase (62). Considering the conservation between aminopeptidase catalytic sites, it will be important to examine whether first- and second-generation PIs modify surface aminopeptidase activities, as well as other peptidases, in each subcellular compartment and affect the biological functions of these enzymes. Finally, because various cell subsets present different levels of peptidase activities (26), it will be necessary to assess the effect of PIs not only on PBMCs, but also on specific cell subsets.

We showed that alteration of proteasome and aminopeptidase activities by HIV PIs modified both the degradation patterns of long HIV peptides and the sensitivity of epitopes to intracellular degradation before loading onto MHC-I, and therefore the amount of peptides available for display to CTL. The effect was both drug and sequence dependent. Variations in degradation patterns were

explained by the intriguing observation that the cleavage of specific residues was enhanced, whereas others were reduced. Twelve residues whose cleavage was reduced by four drugs corresponded to residues cleavable by aminopeptidases, thus suggesting that HIV PIs may reduce the efficiency of aminopeptidase-dependent trimming of many N-extended peptides into epitopes. Surprisingly, these four drugs enhanced the cleavage of acidic residues, mostly E and, to some extent, D, H, Q, which are poorly cleavable by aminopeptidases. Sequential incubation of cells with ritonavir or Kaletra followed by aminopeptidase inhibitor reduced PI-enhanced cleavage of E by 53–59%, suggesting that PI modified aminopeptidase activities to facilitate the cleavage of acidic residues but also enhanced another unidentified peptidase activity. Ritonavir or Kaletra did not enhance caspase-like activity of the proteasome or the activity of caspases (which can cleave motifs containing acidic residues), at least when measured with a pan-caspase substrate (63) (Supplemental Fig. 1), thus ruling out a major involvement of proteasomes and caspases in the changes in residue-specific cleavage patterns. Whether HIV PIs enhance additional cytosolic peptidases cleaving acidic residues or whether it may modify aminopeptidase hydrolytic capacity to enhance cleavage of acidic residues and reduce cleavage of other residues remains to be determined.

These findings have implications for the degradation of HIV proteins and beyond. First, in the context of HIV protein degradation, specifically relevant for HIV-infected, ART-treated persons with ongoing replication of drug-resistant mutated strains, we have shown that HLA-restricted mutations flanking residues tend to evolve from aminopeptidase-cleavable to poorly cleavable residues (24). In the presence of HIV PIs such as Kaletra used as booster in ART treatments, we may expect that the production of the wild type (WT) peptide would be decreased, whereas flanking mutations leading to an acidic residue would enhance epitope production as shown in this study with an isoleucine-to-glutamic acid mutation. Alternatively, a mutation toward an acidic residue within an epitope could enhance the intracellular degradation of the mutated epitope and the production of the WT version. Overall, these changes could affect the ratio of HIV peptides presented by infected cells. Mutated epitopes can elicit CTL responses (64–66); thus, the change of ratio of WT and mutated peptides could contribute to shifts in immunodominance, as seen after immune escape in acute HIV infection (67–70). Although the lack of appropriate longitudinal clinical samples precludes us to test this hypothesis, PI-induced modification of epitope landscape may contribute to broadening of immune responses against HIV in ART-treated patients with ongoing viral replication. In addition, studying the impact of PI on HIV epitope presentation is relevant to approaches to purge HIV reservoirs by combining provirus reactivation in the presence of ART to prevent replication, and therapeutic vaccination to boost immune responses against HIV (71, 72). If ART needed to prevent replication after provirus reactivation calls for inclusion of HIV PIs, it will be important to assess the repertoire of HIV epitopes presented in the context of these therapeutic strategies to define the complementary vaccination strategy better suited to clear reservoirs.

Second, because certain PIs modify Ag processing in a sequence-specific manner, the effect will likely be observed for the degradation of host proteins or proteins derived from other pathogens. The cytosolic stability of optimal epitopes derived from CMV, HCV, influenza, or EBV was variably affected by PI treatment, with ritonavir/Kaletra increasing the cytosolic stability of several peptides (G. Kourjian, unpublished observations). Because intracellular peptide stability contributes to the amount of peptides displayed to CTL (18), HIV PIs may alter the presentation of epitopes derived from other pathogens infecting ART-treated persons. More than half

of HIV[+] individuals worldwide become coinfected with other pathogens such as tuberculosis or HCV, and effective drug combinations to curb both infections are needed (73–75). Assessing whether and how ART, beyond reducing HIV viral load and cellular activation, may possibly contribute to diversifying immune responses against coinfecting pathogens by modifying the degradation patterns of these pathogens provides a new outlook of the use of HIV PIs. Similarly, saquinavir, ritonavir, and nelfinavir, because of their inhibitory effect on the proteasome and other cellular targets, have been shown in previous studies and clinical trials to have beneficial effects on several cancers (31, 34, 76–81). In the repositioning of PIs as cancer therapy, another potential benefit could be a PI-induced altered processing of cancer Ags (the intracellular stability of an MAGE3 epitope was modified by ritonavir/Kaletra; G. Kourjian, unpublished observations), potentially leading to presentation of a different cancer Ag-derived peptide and new immune responses.

Our results indicate that HIV PIs, by altering several cellular peptidase activities, modify Ag processing and epitope presentation. Additional structural studies are needed to understand how HIV PIs modify peptide hydrolytic activity and specificity. However, if HIV PIs allow diversification of epitope presentation, they may provide complementary approaches to treat various immune diseases, considering that temporary PI treatment would not induce toxicity and adverse effects observed in long-term HAART.

Acknowledgments

Disclosures

References
1. Autran, B., G. Carcelain, T. S. Li, C. Blanc, D. Mathez, R. Tubiana, C. Katlama, P. Debré, and J. Leibowitch. 1997. Positive effects of combined antiretroviral therapy on CD4+ T cell homeostasis and function in advanced HIV disease. *Science* 277: 112–116.
2. Flexner, C. 1998. HIV-protease inhibitors. *N. Engl. J. Med.* 338: 1281–1292.
3. Fernández-Montero, J. V., P. Barreiro, and V. Soriano. 2009. HIV protease inhibitors: recent clinical trials and recommendations on use. *Expert Opin. Pharmacother.* 10: 1615–1629.
4. Carr, A., K. Samaras, S. Burton, M. Law, J. Freund, D. J. Chisholm, and D. A. Cooper. 1998. A syndrome of peripheral lipodystrophy, hyperlipidaemia and insulin resistance in patients receiving HIV protease inhibitors. *AIDS* 12: F51–F58.
5. Ena, J., C. Benito, P. Llácer, F. Pasquau, and C. Amador. 2004. [Abnormal body fat distribution and type of antiretroviral therapy as predictors of cardiovascular disease risk in HIV-infected patients]. *Med. Clin. (Barc.)* 122: 721–726.
6. Yarasheski, K. E., P. Tebas, C. Sigmund, S. Dagogo-Jack, A. Bohrer, J. Turk, P. A. Halban, P. E. Cryer, and W. G. Powderly. 1999. Insulin resistance in HIV protease inhibitor-associated diabetes. *J. Acquir. Immune Defic. Syndr.* 21: 209–216.
7. Brown, T. T., and R. B. Qaqish. 2006. Antiretroviral therapy and the prevalence of osteopenia and osteoporosis: a meta-analytic review. *AIDS* 20: 2165–2174.
8. Boesecke, C., and D. A. Cooper. 2008. Toxicity of HIV protease inhibitors: clinical considerations. *Curr. Opin. HIV AIDS* 3: 653–659.
9. Orkin, C., E. DeJesus, H. Khanlou, A. Stoehr, K. Supparatpinyo, E. Lathouwers, E. Lefebvre, M. Opsomer, T. Van de Casteele, and F. Tomaka. 2013. Final 192-week efficacy and safety of once-daily darunavir/ritonavir compared with lopinavir/ritonavir in HIV-1-infected treatment-naïve patients in the ARTEMIS trial. *HIV Med.* 14: 49–59.
10. Erickson, J., D. J. Neidhart, J. VanDrie, D. J. Kempf, X. C. Wang, D. W. Norbeck, J. J. Plattner, J. W. Rittenhouse, M. Turon, N. Wideburg, et al. 1990. Design, activity, and 2.8 A crystal structure of a C2 symmetric inhibitor complexed to HIV-1 protease. *Science* 249: 527–533.
11. Diez-Rivero, C. M., E. M. Lafuente, and P. A. Reche. 2010. Computational analysis and modeling of cleavage by the immunoproteasome and the constitutive proteasome. *BMC Bioinformatics* 11: 479.
12. Goldberg, A. L. 2003. Protein degradation and protection against misfolded or damaged proteins. *Nature* 426: 895–899.
13. York, I. A., A. X. Mo, K. Lemerise, W. Zeng, Y. Shen, C. R. Abraham, T. Saric, A. L. Goldberg, and K. L. Rock. 2003. The cytosolic endopeptidase, thimet

oligopeptidase, destroys antigenic peptides and limits the extent of MHC class I antigen presentation. *Immunity* 18: 429–440.

14. Saric, T., C. I. Graef, and A. L. Goldberg. 2004. Pathway for degradation of peptides generated by proteasomes: a key role for thimet oligopeptidase and other metallopeptidases. *J. Biol. Chem.* 279: 46723–46732.

15. Kawahara, M., I. A. York, A. Hearn, D. Farfan, and K. L. Rock. 2009. Analysis of the role of tripeptidyl peptidase II in MHC class I antigen presentation in vivo. *J. Immunol.* 183: 6069–6077.

16. Serwold, T., F. Gonzalez, J. Kim, R. Jacob, and N. Shastri. 2002. ERAAP customizes peptides for MHC class I molecules in the endoplasmic reticulum. *Nature* 419: 480–483.

17. York, I. A., S. C. Chang, T. Saric, J. A. Keys, J. M. Favreau, A. L. Goldberg, and K. L. Rock. 2002. The ER aminopeptidase ERAP1 enhances or limits antigen presentation by trimming epitopes to 8-9 residues. *Nat. Immunol.* 3: 1177–1184.

18. Lazaro, E., C. Kadie, P. Stamegna, S. C. Zhang, P. Gourdain, N. Y. Lai, M. Zhang, S. A. Martinez, D. Heckerman, and S. Le Gall. 2011. Variable HIV peptide stability in human cytosol is critical to epitope presentation and immune escape. *J. Clin. Invest.* 121: 2480–2492.

19. Herberts, C. A., J. J. Neijssen, J. de Haan, L. Janssen, J. W. Drijfhout, E. A. Reits, and J. J. Neefjes. 2006. Cutting edge: HLA-B27 acquires many N-terminal dibasic peptides: coupling cytosolic peptide stability to antigen presentation. *J. Immunol.* 176: 2697–2701.

20. Reits, E., A. Griekspoor, J. Neijssen, T. Groothuis, K. Jalink, P. van Veelen, H. Janssen, J. Calafat, J. W. Drijfhout, and J. Neefjes. 2003. Peptide diffusion, protection, and degradation in nuclear and cytoplasmic compartments before antigen presentation by MHC class I. *Immunity* 18: 97–108.

21. Kisselev, A. F., T. N. Akopian, K. M. Woo, and A. L. Goldberg. 1999. The sizes of peptides generated from protein by mammalian 26 and 20 S proteasomes. Implications for understanding the degradative mechanism and antigen presentation. *J. Biol. Chem.* 274: 3363–3371.

22. Hearn, A., I. A. York, and K. L. Rock. 2009. The specificity of trimming of MHC class I-presented peptides in the endoplasmic reticulum. *J. Immunol.* 183: 5526–5536.

23. Schatz, M. M., B. Peters, N. Akkad, N. Ullrich, A. N. Martinez, O. Carroll, S. Bulik, H. G. Rammensee, P. van Endert, H. G. Holzhütter, et al. 2008. Characterizing the N-terminal processing motif of MHC class I ligands. *J. Immunol.* 180: 3210–3217.

24. Zhang, S. C., E. Martin, M. Shimada, S. B. Godfrey, J. Fricke, S. Locastro, N. Y. Lai, P. Liebesny, J. M. Carlson, C. J. Brumme, et al. 2012. Aminopeptidase substrate preference affects HIV epitope presentation and predicts immune escape patterns in HIV-infected individuals. *J. Immunol.* 188: 5924–5934.

25. Le Gall, S., P. Stamegna, and B. D. Walker. 2007. Portable flanking sequences modulate CTL epitope processing. *J. Clin. Invest.* 117: 3563–3575.

26. Lazaro, E., S. B. Godfrey, P. Stamegna, T. Ogbechie, C. Kerrigan, M. Zhang, B. D. Walker, and S. Le Gall. 2009. Differential HIV epitope processing in monocytes and CD4 T cells affects cytotoxic T lymphocyte recognition. *J. Infect. Dis.* 200: 236–243.

27. Rock, K. L., C. Gramm, L. Rothstein, K. Clark, R. Stein, L. Dick, D. Hwang, and A. L. Goldberg. 1994. Inhibitors of the proteasome block the degradation of most cell proteins and the generation of peptides presented on MHC class I molecules. *Cell* 78: 761–771.

28. York, I. A., M. A. Brehm, S. Zendzian, C. F. Towne, and K. L. Rock. 2006. Endoplasmic reticulum aminopeptidase 1 (ERAP1) trims MHC class I-presented peptides in vivo and plays an important role in immunodominance. *Proc. Natl. Acad. Sci. USA* 103: 9202–9207.

29. Blanchard, N., T. Kanaseki, H. Escobar, F. Delebecque, N. A. Nagarajan, E. Reyes-Vargas, D. K. Crockett, D. H. Raulet, J. C. Delgado, and N. Shastri. 2010. Endoplasmic reticulum aminopeptidase associated with antigen processing defines the composition and structure of MHC class I peptide repertoire in normal and virus-infected cells. *J. Immunol.* 184: 3033–3042.

30. André, P., M. Groettrup, P. Klenerman, R. de Giuli, B. L. Booth, Jr., V. Cerundolo, M. Bonneville, F. Jotereau, R. M. Zinkernagel, and V. Lotteau. 1998. An inhibitor of HIV-1 protease modulates proteasome activity, antigen presentation, and T cell responses. *Proc. Natl. Acad. Sci. USA* 95: 13120–13124.

31. Gaedicke, S., E. Firat-Geier, O. Constantiniu, M. Lucchiari-Hartz, M. Freudenberg, C. Galanos, and G. Niedermann. 2002. Antitumor effect of the human immunodeficiency virus protease inhibitor ritonavir: induction of tumor-cell apoptosis associated with perturbation of proteasomal proteolysis. *Cancer Res.* 62: 6901–6908.

32. Kelleher, A. D., B. L. Booth, Jr., A. K. Sewell, A. Oxenius, V. Cerundolo, A. J. McMichael, R. E. Phillips, and D. A. Price. 2001. Effects of retroviral protease inhibitors on proteasome function and processing of HIV-derived MHC class I-restricted cytotoxic T lymphocyte epitopes. *AIDS Res. Hum. Retroviruses* 17: 1063–1066.

33. Piccinini, M., M. T. Rinaudo, A. Anselmino, B. Buccinnà, C. Ramondetti, A. Dematteis, E. Ricotti, L. Palmisano, M. Mostert, and P. A. Tovo. 2005. The HIV protease inhibitors nelfinavir and saquinavir, but not a variety of HIV reverse transcriptase inhibitors, adversely affect human proteasome function. *Antivir. Ther. (Lond.)* 10: 215–223.

34. Pajonk, F., J. Himmelsbach, K. Riess, A. Sommer, and W. H. McBride. 2002. The human immunodeficiency virus (HIV)-1 protease inhibitor saquinavir inhibits proteasome function and causes apoptosis and radiosensitization in non-HIV-associated human cancer cells. *Cancer Res.* 62: 5230–5235.

35. Hill, A., W. McBride, A. W. Sawyer, N. Clumeck, and R. K. Gupta. 2013. Resistance at virological failure using boosted protease inhibitors versus non-nucleoside reverse transcriptase inhibitors as first-line antiretroviral therapy—implications for sustained efficacy of ART in resource-limited settings. *J. Infect. Dis.* 207(Suppl. 2): S78–S84.

36. Hosseinipour, M. C., R. K. Gupta, G. Van Zyl, J. J. Eron, and J. B. Nachega. 2013. Emergence of HIV drug resistance during first- and second-line antiretroviral therapy in resource-limited settings. *J. Infect. Dis.* 207(Suppl. 2): S49–S56.

37. Kisselev, A. F., and A. L. Goldberg. 2005. Monitoring activity and inhibition of 26S proteasomes with fluorogenic peptide substrates. *Methods Enzymol.* 398: 364–378.

38. Gourdain, P., J. Boucau, G. Kourjian, N. Y. Lai, E. Duong, and S. Le Gall. 2013. A real-time killing assay to follow viral epitope presentation to CD8 T cells. *J. Immunol. Methods* 398–399: 60–67.

39. Acosta, E. P., T. N. Kakuda, R. C. Brundage, P. L. Anderson, and C. V. Fletcher. 2000. Pharmacodynamics of human immunodeficiency virus type 1 protease inhibitors. *Clin. Infect. Dis.* 30(Suppl. 2): S151–S159.

40. Cardiello, P. G., T. Monnaphol, A. Mahanontharit, R. P. van Heeswijk, D. Burger, A. Hill, K. Ruxrungtham, J. M. Lange, D. A. Cooper, and P. Phanuphak. 2003. Pharmacokinetics of once-daily saquinavir hard-gelatin capsules and saquinavir soft-gelatin capsules boosted with ritonavir in HIV-1-infected subjects. *J. Acquir. Immune Defic. Syndr.* 32: 375–379.

41. Hennessy, M., S. Clarke, J. P. Spiers, D. Kelleher, F. Mulcahy, P. Hoggard, D. Back, and M. Barry. 2004. Intracellular accumulation of nelfinavir and its relationship to P-glycoprotein expression and function in HIV-infected patients. *Antivir. Ther. (Lond.)* 9: 115–122.

42. Jackson, A., V. Watson, D. Back, S. Khoo, N. Liptrott, D. Egan, K. Gedela, C. Higgs, R. Abbas, B. Gazzard, and M. Boffito. 2011. Plasma and intracellular pharmacokinetics of darunavir/ritonavir once daily and raltegravir once and twice daily in HIV-infected individuals. *J. Acquir. Immune Defic. Syndr.* 58: 450–457.

43. van Heeswijk, R. P., A. I. Veldkamp, J. W. Mulder, P. L. Meenhorst, J. M. Lange, J. H. Beijnen, and R. M. Hoetelmans. 2000. Once-daily dosing of saquinavir and low-dose ritonavir in HIV-1-infected individuals: a pharmacokinetic pilot study. *AIDS* 14: F103–F110.

44. Reits, E., J. Neijssen, C. Herberts, W. Benckhuijsen, L. Janssen, J. W. Drijfhout, and J. Neefjes. 2004. A major role for TPPII in trimming proteasomal degradation products for MHC class I antigen presentation. *Immunity* 20: 495–506.

45. Frahm, N., B. Baker, and C. Brander. 2008. Identification and optimal definition of HIV-derived cytotoxic T lymphocyte (CTL) epitopes for the study of CTL escape, functional avidity and viral evolution. In *HIV Molecular Immunology 2008.* B. T. Korber, C. Brander, and B. F. Haynes, et al., eds. Los Alamos National Laboratory, Los Alamos, NM, p. 1–24.

46. Batchelor, R. H., and M. Zhou. 2004. Use of cellular glucose-6-phosphate dehydrogenase for cell quantitation: applications in cytotoxicity and apoptosis assays. *Anal. Biochem.* 329: 35–42.

47. Rosenblum, J. S., and J. W. Kozarich. 2003. Prolyl peptidases: a serine protease subfamily with high potential for drug discovery. *Curr. Opin. Chem. Biol.* 7: 496–504.

48. Schmidtke, G., H. G. Holzhütter, M. Bogyo, N. Kairies, M. Groll, R. de Giuli, S. Emch, and M. Groettrup. 1999. How an inhibitor of the HIV-I protease modulates proteasome activity. *J. Biol. Chem.* 274: 35734–35740.

49. Sato, A., T. Asano, K. Ito, and T. Asano. 2012. Ritonavir interacts with bortezomib to enhance protein ubiquitination and histone acetylation synergistically in renal cancer cells. *Urology* 79:966.e13-21.

50. Ruschak, A., and L. E. Kay. 2012. Proteasome allostery as a population shift between interchanging conformers. *Proc. Natl. Acad. Sci. USA* 109: E3454–E3462.

51. Jankowska, E., M. Gaczynska, P. Osmulski, E. Sikorska, R. Rostankowski, S. Madabhushi, M. Tokmina-Lukaszewska, and F. Kasprzykowski. 2010. Potential allosteric modulators of the proteasome activity. *Biopolymers* 93: 481–495.

52. Kisselev, A. F., T. N. Akopian, V. Castillo, and A. L. Goldberg. 1999. Proteasome active sites allosterically regulate each other, suggesting a cyclical bite-chew mechanism for protein breakdown. *Mol. Cell* 4: 395–402.

53. Spector, A. A. 2006. HIV protease inhibitors and hyperlipidemia: a fatty acid connection. *Arterioscler. Thromb. Vasc. Biol.* 26: 7–9.

54. Anuurad, E., A. Bremer, and L. Berglund. 2010. HIV protease inhibitors and obesity. *Curr. Opin. Endocrinol. Diabetes Obes.* 17: 478–485.

55. Noor, M. A., O. P. Flint, J. F. Maa, and R. A. Parker. 2006. Effects of atazanavir/ritonavir and lopinavir/ritonavir on glucose uptake and insulin sensitivity: demonstrable differences in vitro and clinically. *AIDS* 20: 1813–1821.

56. Waring, J. F., R. Ciurlionis, K. Marsh, L. L. Klein, D. A. Degoey, J. T. Randolph, B. Spear, and D. J. Kempf. 2010. Identification of proteasome gene regulation in a rat model for HIV protease inhibitor-induced hyperlipidemia. *Arch. Toxicol.* 84: 263–270.

57. Lum, P. Y., Y. D. He, J. G. Slatter, J. F. Waring, N. Zelinsky, G. Cavet, X. Dai, O. Fong, R. Gum, L. Jin, et al. 2007. Gene expression profiling of rat liver reveals a mechanistic basis for ritonavir-induced hyperlipidemia. *Genomics* 90: 464–473.

58. Meiners, S., D. Heyken, A. Weller, A. Ludwig, K. Stangl, P. M. Kloetzel, and E. Krüger. 2003. Inhibition of proteasome activity induces concerted expression of proteasome genes and de novo formation of Mammalian proteasomes. *J. Biol. Chem.* 278: 21517–21525.

59. Riddle, T. M., D. G. Kuhel, L. A. Woollett, C. J. Fichtenbaum, and D. Y. Hui. 2001. HIV protease inhibitor induces fatty acid and sterol biosynthesis in liver and adipose tissues due to the accumulation of activated sterol regulatory element-binding proteins in the nucleus. *J. Biol. Chem.* 276: 37514–37519.

60. Kramer, W., F. Girbig, D. Corsiero, A. Pfenninger, W. Frick, G. Jähne, M. Rhein, W. Wendler, F. Lottspeich, E. O. Hochleitner, et al. 2005. Aminopeptidase N (CD13) is a molecular target of the cholesterol absorption inhibitor ezetimibe in the enterocyte brush border membrane. *J. Biol. Chem.* 280: 1306–1320.

61. Levy, E., S. Spahis, D. Sinnett, N. Peretti, F. Maupas-Schwalm, E. Delvin, M. Lambert, and M. A. Lavoie. 2007. Intestinal cholesterol transport proteins: an update and beyond. *Curr. Opin. Lipidol.* 18: 310–318.

62. Yeh, T. Y., J. I. Sbodio, Z. Y. Tsun, B. Luo, and N. W. Chi. 2007. Insulin-stimulated exocytosis of GLUT4 is enhanced by IRAP and its partner tankyrase. *Biochem. J.* 402: 279–290.

63. Thornberry, N. A., T. A. Rano, E. P. Peterson, D. M. Rasper, T. Timkey, M. Garcia-Calvo, V. M. Houtzager, P. A. Nordstrom, S. Roy, J. P. Vaillancourt, et al. 1997. A combinatorial approach defines specificities of members of the caspase family and granzyme B. Functional relationships established for key mediators of apoptosis. *J. Biol. Chem.* 272: 17907–17911.

64. Feeney, M. E., Y. Tang, K. Pfafferott, K. A. Roosevelt, R. Draenert, A. Trocha, X. G. Yu, C. Verrill, T. Allen, C. Moore, et al. 2005. HIV-1 viral escape in infancy followed by emergence of a variant-specific CTL response. *J. Immunol.* 174: 7524–7530.

65. Allen, T. M., X. G. Yu, E. T. Kalife, L. L. Reyor, M. Lichterfeld, M. John, M. Cheng, R. L. Allgaier, S. Mui, N. Frahm, et al. 2005. De novo generation of escape variant-specific CD8+ T-cell responses following cytotoxic T-lymphocyte escape in chronic human immunodeficiency virus type 1 infection. *J. Virol.* 79: 12952–12960.

66. O'Connell, K. A., R. W. Hegarty, R. F. Siliciano, and J. N. Blankson. 2011. Viral suppression of multiple escape mutants by de novo CD8(+) T cell responses in a human immunodeficiency virus-1 infected elite suppressor. *Retrovirology* 8: 63.

67. Turnbull, E. L., M. Wong, S. Wang, X. Wei, N. A. Jones, K. E. Conrod, D. Aldam, J. Turner, P. Pellegrino, B. F. Keele, et al. 2009. Kinetics of expansion of epitope-specific T cell responses during primary HIV-1 infection. *J. Immunol.* 182: 7131–7145.

68. Liu, M. K., N. Hawkins, A. J. Ritchie, V. V. Ganusov, V. Whale, S. Brackenridge, H. Li, J. W. Pavlicek, F. Cai, M. Rose-Abrahams, et al; CHAVI Core B. 2013. Vertical T cell immunodominance and epitope entropy determine HIV-1 escape. *J. Clin. Invest.* 123: 380–393.

69. Borrow, P., H. Lewicki, X. Wei, M. S. Horwitz, N. Peffer, H. Meyers, J. A. Nelson, J. E. Gairin, B. H. Hahn, M. B. Oldstone, and G. M. Shaw. 1997. Antiviral pressure exerted by HIV-1-specific cytotoxic T lymphocytes (CTLs) during primary infection demonstrated by rapid selection of CTL escape virus. *Nat. Med.* 3: 205–211.

70. Nowak, M. A., R. M. May, R. E. Phillips, S. Rowland-Jones, D. G. Lalloo, S. McAdam, P. Klenerman, B. Köppe, K. Sigmund, C. R. Bangham, et al. 1995. Antigenic oscillations and shifting immunodominance in HIV-1 infections. *Nature* 375: 606–611.

71. Archin, N. M., A. L. Liberty, A. D. Kashuba, S. K. Choudhary, J. D. Kuruc, A. M. Crooks, D. C. Parker, E. M. Anderson, M. F. Kearney, M. C. Strain, et al. 2012. Administration of vorinostat disrupts HIV-1 latency in patients on antiretroviral therapy. *Nature* 487: 482–485.

72. Siliciano, J. D., and R. F. Siliciano. 2013. HIV-1 eradication strategies: design and assessment. *Curr. Opin. HIV AIDS* 8: 318–325.

73. Jalali, Z., and J. K. Rockstroh. 2012. Antiviral drugs and the treatment of hepatitis C. *Curr. HIV/AIDS Rep.* 9: 132–138.

74. Naidoo, K., C. Baxter, and S. S. Abdool Karim. 2013. When to start antiretroviral therapy during tuberculosis treatment? *Curr. Opin. Infect. Dis.* 26: 35–42.

75. Walker, N. F., G. Meintjes, and R. J. Wilkinson. 2013. HIV-1 and the immune response to TB. *Future Virol.* 8: 57–80.

76. Bono, C., L. Karlin, S. Harel, E. Mouly, S. Labaume, L. Galicier, S. Apcher, H. Sauvageon, J. P. Fermand, J. C. Bories, and B. Arnulf. 2012. The human immunodeficiency virus-1 protease inhibitor nelfinavir impairs proteasome activity and inhibits the proliferation of multiple myeloma cells in vitro and in vivo. *Haematologica* 97: 1101–1109.

77. Kawabata, S., J. J. Gills, J. R. Mercado-Matos, J. Lopiccolo, W. Wilson, III, M. C. Hollander, and P. A. Dennis. 2012. Synergistic effects of nelfinavir and bortezomib on proteotoxic death of NSCLC and multiple myeloma cells. *Cell Death Dis.* 3: e353.

78. Kraus, M., E. Malenke, J. Gogel, H. Müller, T. Rückrich, H. Overkleeft, H. Ovaa, E. Koscielniak, J. T. Hartmann, and C. Driessen. 2008. Ritonavir induces endoplasmic reticulum stress and sensitizes sarcoma cells toward bortezomib-induced apoptosis. *Mol. Cancer Ther.* 7: 1940–1948.

79. Sgadari, C., P. Monini, G. Barillari, and B. Ensoli. 2003. Use of HIV protease inhibitors to block Kaposi's sarcoma and tumour growth. *Lancet Oncol.* 4: 537–547.

80. Zeng, J., A. P. See, K. Aziz, S. Thiyagarajan, T. Salih, R. P. Gajula, M. Armour, J. Phallen, S. Terezakis, L. Kleinberg, et al. 2011. Nelfinavir induces radiation sensitization in pituitary adenoma cells. *Cancer Biol. Ther.* 12: 657–663.

81. Kimple, R. J., A. V. Vaseva, A. D. Cox, K. M. Baerman, B. F. Calvo, J. E. Tepper, J. M. Shields, and C. I. Sartor. 2010. Radiosensitization of epidermal growth factor receptor/HER2-positive pancreatic cancer is mediated by inhibition of Akt independent of ras mutational status. *Clin. Cancer Res.* 16: 912–923.